Biochimica et Biophysica Acta 1808 (2011) 1772–1778

Contents lists available at ScienceDirect

Biochimica et Biophysica Acta

journal homepage: www.elsevier.com/locate/bbamem

Extracellular K^+ elevates outward currents through Kir2.1 channels by increasing single-channel conductance

Tai-An Liu, Hsueh-Kai Chang, Ru-Chi Shieh *

Institute of Biomedical Sciences, Academia Sinica, Taipei 11529, Taiwan, ROC

ARTICLE INFO

Article history:
Received 27 January 2011
Received in revised form 17 February 2011
Accepted 22 February 2011
Available online 1 March 2011

Keywords:
Inward-rectification
Permeation
Kinetics
Excitability

ABSTRACT

Outward currents through inward rectifier K^+ channels (Kir) play a pivotal role in determining resting membrane potential and in controlling excitability in many cell types. Thus, the regulation of outward Kir current (I_{K1}) is important for appropriate physiological functions. It is known that outward I_{K1} increases with increasing extracellular K^+ concentration ($[K^+]_o$), but the underlying mechanism is not fully understood. A "K^+-activation of K^+-channel" hypothesis and a "blocking-particle" model have been proposed to explain the $[K^+]_o$-dependence of outward I_{K1}. Yet, these mechanisms have not been examined at the single-channel level. In the present study, we explored the mechanisms that determine the amplitudes of outward I_{K1} at constant driving forces [membrane potential (V_m) minus reversal potential (E_K)]. We found that increases in $[K^+]_o$ elevated the single-channel current to the same extent as macroscopic I_{K1} but did not affect the channel open probability at a constant driving force. In addition, spermine-binding kinetics remained unchanged when $[K^+]_o$ ranged from 1 to 150 mM at a constant driving force. We suggest the regulation of K^+ permeation by $[K^+]_o$ as a new mechanism for the $[K^+]_o$-dependence of outward I_{K1}.

1. Introduction

Outward currents passing through Kir channels play crucial roles in controlling membrane excitability and action potential duration in many cell types. When $[K^+]_o$ is increased, the outward I_{K1} increases in a driving force dependent manner [1–6]. Because the outward I_{K1} plays a pivotal role in determining the action potential threshold, increases in outward I_{K1} cause reduced excitability and slower conductance. The $[K^+]_o$-dependence of outward I_{K1} is thus important in regulating cellular physiological and pathological functions.

Two mechanisms have been proposed to explain the $[K^+]_o$-dependence of outward I_{K1}. First, the "K^+-activation of K^+-channel" hypothesis suggests that extracellular K^+ interacts with Kir channels and subsequently increases channel open probability [4,7,8]. Direct activation of K^+ channels by K^+ has been proposed as an explanation for the increase in K^+ channel activity (in various types of K^+ channels) caused by increased $[K^+]_o$ [4,7–10]. It has been shown that Kir1.1 channels are activated by $[K^+]_o$ in the millimolar range [11,12] and that this K^+-dependent gating is linking to pH gating through a conformational change in the pore [13]. In addition, site-directed mutagenesis has suggested that K^+ occupancy of extracellular site(s) is involved in the K^+ activation of inward rectifier K^+ channels and V_m-gated K^+ channels [4,7,9,14]. Furthermore, it has been suggested that extracellular K^+ may affect the number of functional Kir1.1 and K_v1.4 channels [10,12]. However, the effects of extracellular K^+ on the single-channel kinetics of the Kir channel are not yet clear.

The other hypothesis, the blocking-particle model, proposes that extracellular K^+ may bind to a high-affinity site in the Kir2.1 channel pore and electrostatically weaken pore blockade by intracellular Mg^{2+} or polyamines, such that inward rectification is weaker at higher $[K^+]_o$ [5,8]. Similar effects of $[K^+]_o$ on intracellular Mg^{2+} blockage have been suggested in work with the K_v channel [15]. Recently, it has been shown, at the single-channel level, that the driving force dependent shifts of I–V_m curves are attributable to the driving force dependence of blocking kinetics when E_K is changed by varying $[K^+]_o$ [6]. However, the role of this mechanism on the $[K^+]_o$-dependence of outward I_{K1} has not been explored at the single-channel level.

In the present study, we investigated these two hypotheses by examining the single-channel kinetics of the Kir2.1 channel, with the aim of explaining the $[K^+]_o$-dependence of outward Kir2.1 currents. We explored whether $[K^+]_o$ modulated single-channel properties, and determined the kinetics of intracellular spermine block of the Kir2.1 channel. Our results show that outward I_{K1} is larger at higher $[K^+]_o$, because single-channel conductance is elevated at higher $[K^+]_o$. In addition, neither channel open probability nor spermine-binding

Abbreviations: Kir, inward rectifier K^+ channels; I_{K1}, Kir2.1 currents; $[K^+]_o$, extracellular K^+ concentration; V_m, membrane potential; k_1, rate constant for the transition from the closed to the open state; k_{-1}, rate constant for the transition from the open to the closed state; μ, the association rate constant for spermine binding; λ, the dissociation rate constant for spermine binding; i_{K1}, single-channel Kir2.1 currents

* Corresponding author at: Institute of Biomedical Sciences, Academia Sinica, 128 Yen-Chiu Yuan Road, Section 2, Taipei 115, Taiwan, ROC. Tel.: +886 2 2652 3914; fax: +886 2 2782 9143.

E-mail address: ruchi@ibms.sinica.edu.tw (R.-C. Shieh).

0005-2736/$ – see front matter © 2011 Elsevier B.V. All rights reserved.
doi:10.1016/j.bbamem.2011.02.016

kinetics were altered at a constant driving force when $[K^+]_o$ was in the range 1–150 mM.

2. Materials and methods

2.1. Preparation of Xenopus oocytes

Xenopus oocytes were isolated by partial ovariectomy from frogs anaesthetized with 0.1% tricaine (3-aminobenzoic acid ethyl ester). After suturing the surgical incision, animals were monitored during the recovery period before being returned to their tank. All surgical and anesthesia procedures were reviewed and approved by the Academia Sinica Institutional Animal Care and Utilization Committee.

2.2. Molecular biology

cRNAs to be expressed in *Xenopus* oocytes were prepared by in vitro transcription (mMessage mMachine, Ambion, Dallas, TX). Site-directed mutations were generated using polymerase chain reaction (PCR). The correctness of mutations was confirmed by sequencing of cDNAs using an ABI Prism™ dRhodamine Terminator Cycle Sequencing Ready Reaction Kit (PE Applied Biosystems, Foster City, CA).

2.3. Electrophysiological recordings

Currents were recorded at room temperature (21 °C–24 °C) using the patch-clamp technique [16,17] and an Axopatch 200B amplifier (Molecular Devices, Sunnyvale, CA). The standard solution (pH 7.4) contained (in mM) KCl, 121; KOH, 20; K_2HPO_4, 4; KH_2PO_4, 1; and EDTA, 5. For giant-patch recordings, the intracellular solution (pH 7.4) contained (in mM) KCl, 76; KOH, 20; K_2HPO_4, 4; KH_2PO_4, 1; KF, 5; EDTA, 5; Na_3VO_4, 0.1; and $K_4P_2O_7$, 10 [18]. For experiments employing giant outside-out patches, the compositions of other solutions (1–20 mM $[K^+]_o$) were (in mM): KCl, 0.3–19.3; KOH, 0.7; HEPES, 1; at pH 7.4. In some experiments (Fig. 1), 280 mM sucrose was added to solutions containing $[K^+]_o \leq 20$ mM to maintain osmolarity. Single-channel recordings were performed using inside-out patches at a sampling rate of 1 kHz and a filtering rate of 0.5 kHz. The intracellular solution (pH 7.4) contained (in mM) KCl, 121; KOH, 20; K_2HPO_4, 4; KH_2PO_4, 1; KF, 5; and EDTA, 5. The 1 mM $[K^+]$ pipette solution contained (in mM): KCl, 0.1; K_2HPO_4, 0.4; KH_2PO_4, 0.1; at pH 7.4. The 20 mM $[K^+]$ pipette solution contained (in mM): KCl, 11; K_2HPO_4, 4; KH_2PO_4, 1; at pH 7.4. Command voltages were controlled and data were acquired using pClamp 10 software (Molecular Devices).

2.4. Data analysis

Single-channel events recorded from separate patches at the same condition were pooled and shown on square root-log coordinates to construct single open and zero-current time distributions, which were best-fitted employing one or two exponential components, using the maximum-likelihood method [19]. Averaged data are presented as means ± SEMs. Student's unpaired *t* test was used to assess the statistical significance of differences, and a *p*-value <0.05 was considered statistically significant.

3. Results

3.1. Increased $[K^+]_o$ elevates outward K^+ conductance

To focus on the effects of extracellular K^+ on outward I_{K1}, we examined $[K^+]_o$-dependence of I_{K1} with K^+ as the only extracellular cation. Fig. 1A shows the I–V_m relationships recorded from one outside-out patch expressing Kir2.1 channels at $[K^+]_o = 1$–150 mM. I–V_m curves were almost linear at V_m negative to E_K. In contrast, at V_m positive to E_K, I_{K1} reached a maximum value, which we refer to as peak outward I_{K1}.

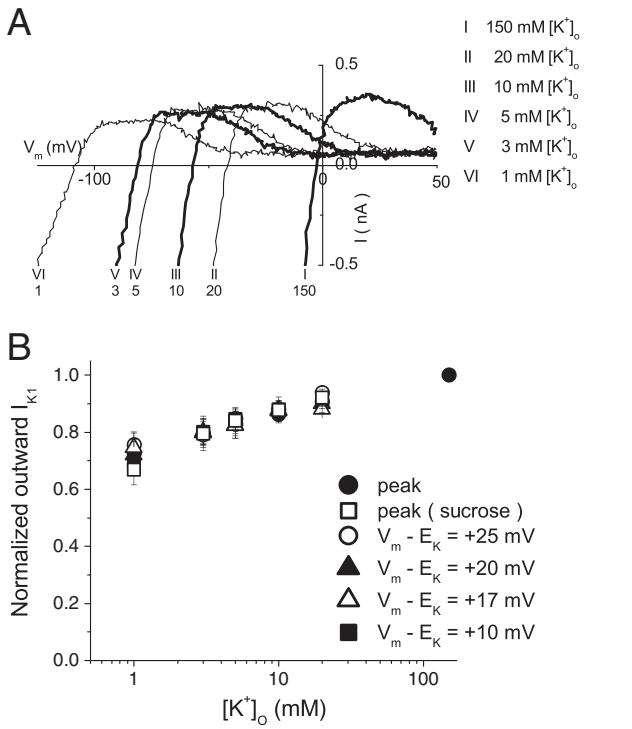

Fig. 1. Effects of extracellular K^+ on the Kir2.1 channel I–V_m relationship. A. I–V_m curves were recorded using a ramp protocol ($V_m = -150$ to $+50$ mV over 3 s) from outside-out patches exposed to the indicated values of $[K^+]_o$, with K^+ as the only extracellular cation. B. Summary of the effects of $[K^+]_o$ on normalized peak outward I_{K1} and normalized outward I_{K1} at driving forces $= +10$, $+17$, $+20$, and $+25$ mV in the Kir2.1 channel. $n = 4$–6.

Fig. 1B shows that the normalized peak outward I_{K1} (I_{K1} at the test $[K^+]_o$ divided by I_{K1} at 150 mM $[K^+]_o$) decreased by 25% (from 1 to 0.75 ± 0.05) when $[K^+]_o$ was reduced from 150 mM to 1 mM. This $[K^+]_o$-dependence of outward I_{K1} was smaller than that previously determined [3] (see Discussion). The shallow $[K^+]_o$-dependence of the peak outward I_{K1} ratio was not due to osmolarity imbalance because $[K^+]_o$-dependence of the peak outward I_{K1} ratio was the same in the presence and absence of sucrose (Fig. 1B). The driving force where peak outward I_{K1} occurred, varied from patch to patch. Because the shape of I_{K1}–V_m relationships depends on driving forces rather than on V_m when $[K^+]_o$ values are varied [1,4–6,20–24], we examined the effects of $[K^+]$ on outward I_{K1} at constant driving forces. Fig. 1B shows that the $[K^+]_o$-dependence of peak outward I_{K1} and outward I_{K1} at driving forces $= +10$, $+17$, $+20$, and $+25$ mV was the same. The results show that the degree of $[K^+]_o$-dependence of outward I_{K1} is not affected by the driving force selected.

Next, we examined how $[K^+]_o$ increases K^+ efflux at the single-channel level. Fig. 2A shows i_{K1} recorded at 20 mM $[K^+]_o$, 150 mM $[K^+]_i$, and $V_m = -28$ mV ($E_K = -45.1 \pm 0.8$ mV, $n = 6$; driving force $= +17$ mV), in the absence of any added intracellular blocker (control, left panel) in an inside-out patch. Open and zero-current time histograms were constructed and are shown in Fig. 2B. The open lifetimes were distributed according to a single exponential function with a mean open time (τ_o) of 207 ms. Zero-current times were described using two exponential functions. The fast mean zero-current time (τ_f) was 3.2 ms and the slow mean zero-current time (τ_s), 120.0 ms. Next, we recorded outward i_{K1} at a driving force $= +17$ mV, 20 mM $[K^+]_o$, and 150 mM $[K^+]_i$, in the presence of a $[\text{spermine}]_i$ concentration of 10 nM (Fig. 2A, right panel). The open lifetimes were distributed according to a single exponential function and τ_o was 35.4 ms (Fig. 2C). The zero-current time histograms could still be represented using two exponential functions (Fig. 2C). The values τ_f was 3.8 ms and τ_s, 119 ms (Fig. 2C). Spermine increased the proportion of

the slow component of all zero-current events from 0.12 to 0.77. These results suggest that the slow component of the zero-current time observed in the control group is probably attributable to residual blockage of the Kir2.1 channel by an intracellular polyamine [25]. To understand how extracellular K^+ affected the kinetics of the single channel in both the absence and presence of an intracellular blocker, we considered a sequential model with one closed state, one open state, and one blocked state as follows:

$$C \underset{k_{-1}}{\overset{k_1}{\rightleftharpoons}} O \underset{\lambda}{\overset{\mu}{\rightleftharpoons}} B \qquad \text{Scheme I,}$$

where C is the closed state, O the open state, and B the blocked state. The same scheme has been used to describe the single-channel transitions in the Kir2.1 channel expressed in COS-1 cells with similar sampling and filtering rates [6]. The transition between the C and O states is termed intrinsic gating [26]. Rate constants are related to τ_o, τ_f, and τ_s, as follows:

$$k_{-1} + \mu \times ([B] + [X]) = 1/\tau_o \tag{1}$$

$$k_1 = 1/\tau_f \tag{2}$$

$$\lambda = 1/\tau_s \tag{3}$$

where $[B]$ and $[X]$ denote the concentrations of added spermine and residual blocker, respectively. To obtain μ, we measured the open times and calculated τ_o in the presence of spermine at $B1$ (1 nM) and $B2$ (10 nM) concentration. From Eq. (1),

$$\mu = 1/\{(B1-B2) \times [1/\tau_o(B1) - 1/\tau_o(B2)]\}. \tag{4}$$

To obtain k_{-1} and $[X]$, we used the probability density function of the zero-current time, described as follows [27]:

$$f(t) = A_s/\tau_s \times e^{-t/\tau_s} + A_f/\tau_f \times e^{-t/\tau_f} \tag{5}$$

where $A_s = k_{-1}/[k_{-1} + \mu\times([B]+[X])]$ and $A_f = \mu\times([B]+[X])/[k_{-1} + \mu\times([B]+[X])]$. $[X]$, the residual $[\text{spermine}]_i$, was estimated to be in the range 0.3–0.5 nM.

To examine whether increases in $[K^+]_o$ could activate the Kir2.1 channel, we determined if/how i_{K1} amplitude, k_1, and k_{-1} were affected by $[K^+]_o$. Fig. 3A shows i_{K1} recorded at 150 mM $[K^+]_o$ ($E_K = -3.0 \pm 0.9$ mV, $n = 3$; left panel) and 1 mM $[K^+]_o$ ($E_K = -109 \pm 0.8$ mV, $n = 5$; right panel), at a driving force = +17 mV, respectively. Fig. 3B shows the corresponding open and zero-current time histograms. The values of τ_o, τ_f, and τ_s were 220 ms, 2.9 ms, and 177 ms at 150 mM $[K^+]_o$, and 257 ms, 3.7 ms, and 128 ms at 1 mM $[K^+]_o$. k_1 and k_{-1} were calculated based on Eqs. (2), (4) and (5). Fig. 3C shows that i_{K1}, k_1 and k_{-1} were larger when $[K^+]_o$ increased. However, open probabilities (P_o) (Fig. 3Cd) were not affected by $[K^+]_o$ at a driving force = +17 mV. Values of k_1 and k_{-1} were not dependent on driving forces (Fig. 3D) but k_1 and k_{-1} slightly increased as V_m became more positive.

Next, we examined the effects of $[K^+]_o$ on single-channel conductance. Fig. 4A shows that the single-channel i_{K1}–V_m relationships at various $[K^+]_o$ were linear. The single-channel conductance calculated from the slope was 35 pS at 150 mM $[K^+]_o$, 32 pS at 20 mM $[K^+]_o$, 30 pS at 5 mM $[K^+]_o$, and 28 pS at 1 mM $[K^+]_o$. Fig. 4B compares the $[K^+]_o$-dependence of normalized single-channel conductance and normalized macroscopic I_{K1} at a driving force = +17 mV. The data show that the $[K^+]_o$-dependence of macroscopic outward I_{K1} at a constant driving force can be attributed to the $[K^+]_o$-dependence of single-channel conductance.

3.2. Effect of $[K^+]_o$ on spermine-binding kinetics

It has been shown that changes in $[K^+]_o$ shift the V_m-dependence of polyamine block [5,6], indicating that the polyamine block can be relieved by K^+ influx. These findings explain why outward I_{K1} depends on driving forces but not on V_m alone when $[K^+]_o$ changes. However, it remained unclear whether blockage of outward I_{K1} by intracellular polyamines was smaller at higher $[K^+]_o$, at a constant driving force, so that i_{K1} increased when $[K^+]_o$ rose. To explore this topic, we determined the effects of $[K^+]_o$ on the association rate constant μ, and the dissociation rate constant λ of spermine block. Single-channel recordings were obtained from inside-out patches at

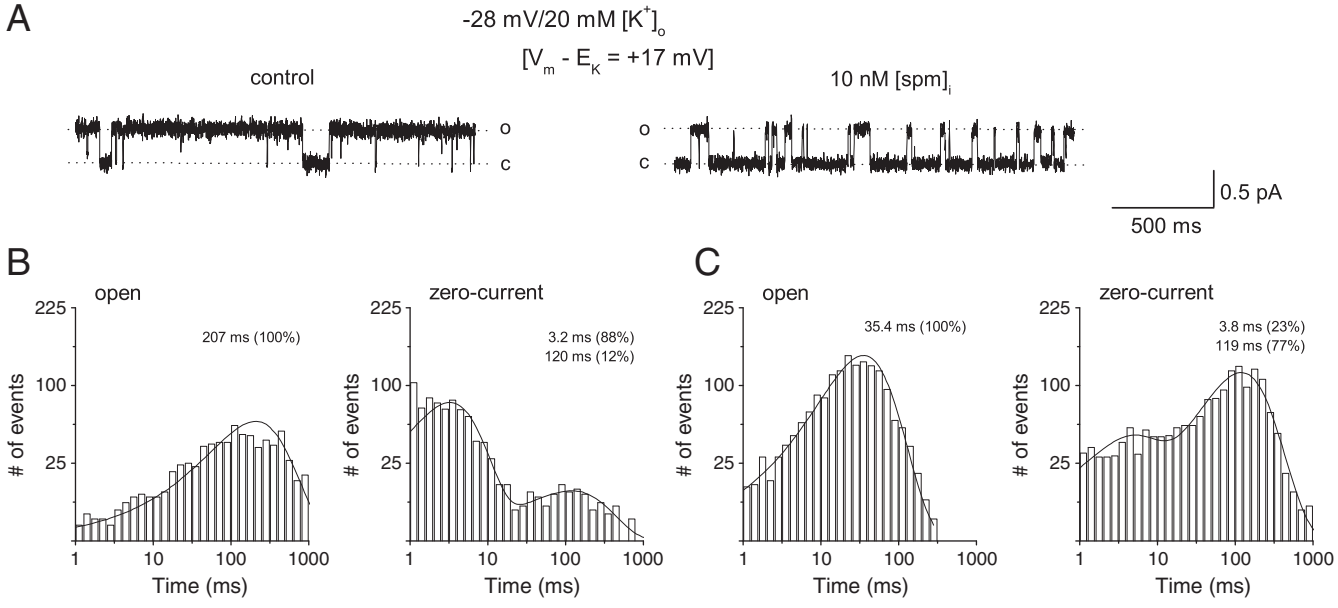

Fig. 2. Effects of intracellular spermine on single-channel i_{K1}. (A) Single-channel currents recorded at 20 mM $[K^+]_o$/150 mM $[K^+]_i$ at $V_m = -28$ mV (driving force = +17 mV) in the absence (left panel) and presence (right panel) of 10 nM $[\text{spermine}]_i$ (right panel). The open and zero-current time distributions of single-channel currents in the absence (B) and presence of 10 nM $[\text{spermine}]_i$ (C) are also shown. Due to small number of total events per patch, all histograms in this study were constructed by pooling single-channel events recorded from separate patches ($n = 3$–7) of the same condition. The mean open and zero-current times obtained by this method have been shown to be similar to those determined by averaging the mean open and mean zero-current times of each patch [34].

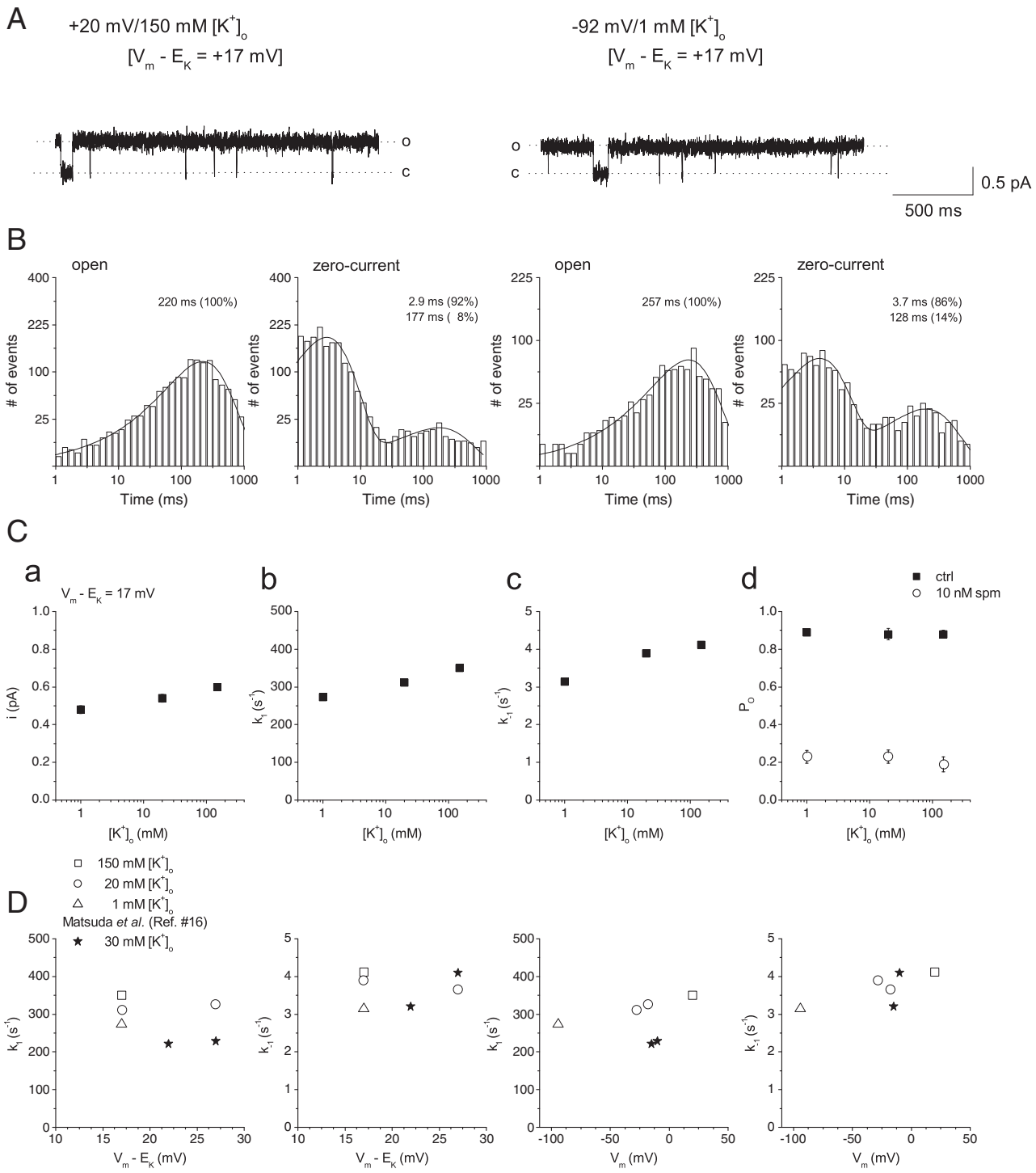

Fig. 3. Effects of $[K^+]_o$ on single-channel i_{K1}. A. Single-channel currents recorded at 150 mM $[K^+]_o$ (left panel) and 1 mM $[K^+]_o$ (right panel) at 150 mM $[K^+]_i$ and driving force = +17 mV without adding spermine. B. The open and zero-current time distributions of single-channel currents. C. Effects of $[K^+]_o$ on i_{K1} (a), k_1 (b), k_{-1} (c), and open probability (d). D. Driving force- and V_m-dependence of k_1 and k_{-1}. The data reported by Matsuda et al., 2010 [6] are shown as closed stars.

$[K^+]_o$ = 1 mM or 150 mM, $[\text{spermine}]_i$ = 10 nM, $[K^+]_i$ = 150 mV, and a driving force = +17 mV (Fig. 5A). Mean open and zero-current times were estimated from the open and zero-current time histograms (Fig. 5B). μ and λ were next calculated using Eqs. (4) and (3). Fig. 5E shows that neither μ nor λ was affected when $[K^+]_o$ was changed at a driving force = +17 mV and thus the open probability in the presence of spermine was not significantly changed by $[K^+]_o$ either (p>0.05; data shown in Fig. 3Cd for comparison with the control). To examine the effects of V_m on μ and λ, single-channel recordings were obtained at $[K^+]_o$ = 20 mM and V_m = −18 mV in the absence and presence of 10 nM $[\text{spermine}]_i$ (Fig. 5C), in addition to those at V_m = −28 mV (Fig. 2A). Figure 5D shows the corresponding open and zero-current histograms at V_m = 18 mV. Fig. 5F shows that, at 20 mM $[K^+]_o$, μ increased and λ decreased when V_m was increased from −28 to −18 mV. In other words, an increase in V_m elevated spermine-binding affinity. Because of the very low P_o (<0.001) at V_m = −8 mV, we could not estimate μ and λ at more positive values of V_m. Assuming that the V_m-dependencies of μ and λ are both Boltzmann relationships, logμ–V_m and logλ–V_m plots should be linear (dotted lines in Fig. 5F). If μ and λ depend only on V_m, thus not on $[K^+]_o$, then

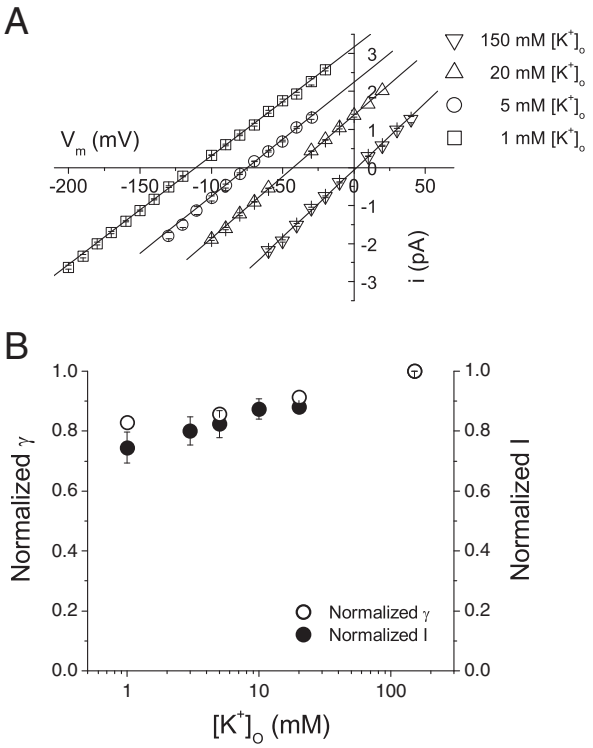

Fig. 4. $[K^+]_o$-dependence of macroscopic I_{K1} and single-channel conductance. A. Relationships of i_{K1}–V_m at $[K^+]_o = 1$–150 mM ($n = 3$–15). B. Summary of the effects of $[K^+]_o$ on normalized I_{K1} and normalized single-channel conductance (γ) at a driving force = +17 mV. I_{K1} and γ were normalized to values obtained at 150 mM $[K^+]_o$.

both the μ and λ values estimated at 1 mM and 150 mM $[K^+]_o$ should be close to the extrapolated dotted line. However, μ was larger than the predicted value at 1 mM $[K^+]_o$ and smaller at 150 mM $[K^+]_o$, whereas λ was lower than expected at 1 mM $[K^+]_o$ and greater at 150 mM $[K^+]_o$ (Fig. 5F). These results suggest that at a constant V_m, an increase in $[K^+]_o$ decreased intracellular spermine block of the Kir2.1 channel, resulting in an increase in outward I_{K1} (Fig. 6, grey vertical arrow). However, when $[K^+]_o$ is changed, it is the dependence of outward I_{K1} on driving forces (Fig. 6, black vertical arrow) but not on V_m that is relevant to the physiological and pathological functions of the Kir2.1 channel. Therefore, we focused on the effects of $[K^+]_o$ on spermine blocking kinetics at the same driving force. The results from Fig. 5 suggest that spermine-binding kinetics depended on driving forces rather than on $[K^+]_o$ per se.

4. Discussion

4.1. The $[K^+]_o$-dependence of outward I_{K1} is attributable to $[K^+]_o$-dependence of single-channel conductance

In the present study, we explored the mechanism underlying the $[K^+]_o$-dependence of outward I_{K1}, which is important in the regulation of physiological and pathological functions of excitable cells. The data show that the macroscopic I_{K1}–$[K^+]_o$ relationship is the same as the single-channel γ–$[K^+]_o$ curve, supporting that K^+ permeation is regulated by $[K^+]_o$. Precisely how $[K^+]_o$ increases the single-channel conductance of the Kir2.1 channel remains unclear. According to the crystal structure of KcsA channels [28,29], extracellular K^+ can change single-channel conductance through its interactions with sites within the selectivity filter. Extracellular K^+ may regulate the conductance of the Kir2.1 channel through a similar mechanism. Because $I = nP_o i$ (where n is the channel number), and because P_o is not affected by $[K^+]_o$ changes (Fig. 3Cd), the same $[K^+]_o$-dependence of I_{K1} and i_{K1} suggests that channel number is probably not affected by changes in $[K^+]_o$. Therefore, the mechanism of increased K^+ conductance in the Kir2.1 channel seems to differ from the activation mode of the Kir1.1b channel and a voltage-dependent K^+ channel, $K_v1.4$. It has been shown that the number of Kir1.1 channels increases when $[K^+]_o$ is increased from 1 to 50 mM but this type of channel activation is not observed in the Kir2.1 channel [12]. In the $K_v1.4$ channel, it has been shown that the single-channel conductance is not affected when $[K^+]_o$ increased, and it is suggested that channel number rose when $[K^+]_o$ is elevated [10].

4.2. Regulation of the spermine block by $[K^+]_o$

Our study suggests that the dependence of outward I_{K1} on $[K^+]_o$ and driving forces (Fig. 6, black vertical arrow) may not be due to regulation of the polyamine block by $[K^+]_o$ per se. The finding is consistent with that of a previous study showing that the binding affinity of spermine, inhibiting outward I_{K1} through the Kir2.1 channel, was the same at different $[K^+]_o$ values when the driving force is kept constant [30]. Furthermore, it has been shown that the Kir2.1 channel remains sensitive to extracellular K^+ level even in the absence of polyamines [31].

Fig. 5E shows that when $[K^+]_o$ was varied, both the association and dissociation rate constants of spermine depended on driving forces. The dependence of the association constant of spermine on driving forces may be due to the concerted movement of spermine and K^+ in the Kir2.1 pore [32]. The dependence of the spermine dissociation rate on driving forces may be explained as follows. A decrease in V_m will tend to pull spermine out of the pore into the intracellular side whereas an increase in $[K^+]_o$ (thus an increased in E_K) can knock off the spermine.

4.3. Comparison with previous studies

Recently, it is shown at the single-channel level that the driving force dependent inward rectification is attributable to the driving force dependence of blocking kinetics when E_K is changed by varying $[K^+]_o$ [6]. The data presented in this study are consistent with this conclusion. Furthermore, the k_{-1}, μ and λ values at 20 mM $[K^+]_o$ shown in this study (Figs. 3D and 5E, hollow symbols) are similar to those at 30 mM $[K^+]_o$ determined by Matsuda et al. (solid symbols) [6]. It may be noted that the theme of our study is different from the previous study [6]. Matsuda et al. [6] focus on the mechanisms underlying the shift of the I–V_m relationship induced by $[K^+]_o$ changes (Fig. 6, the horizontal arrow) whereas our study explores the mechanism for the $[K^+]_o$-dependence of outward I_{K1} amplitude (Fig. 6, black vertical arrow). The different effects of $[K^+]_o$ examined by the previous study [6] and by our study have different physiological implications. The shift of I–V_m relationships changes the resting membrane potential, thus affects the number of available Na^+ channels for activation, and thereby induces variation in electrical excitability of cells. On the other hand, the change of outward I_{K1} amplitude affects the excitability by varying the action potential threshold. The larger the outward I_{K1} is, the larger is the inward Na^+ current required for initiating an action potential. Furthermore, the larger outward I_{K1} will increase repolarization and shorten the action potential duration.

Our single-channel kinetic analysis suggests that a residual intracellular blocking agent ($\approx$ 0.3–0.5 nM) inhibits outward I_{K1} in oocytes. However, it has been shown that residual intracellular blockers are < 0.1 nM in concentration in COS-1 cells [26]. Furthermore, the $[K^+]_o$-dependence of outward I_{K1} reported in this study is much smaller than that previously determined in cardiac myocytes [3]. The reasons for the different degrees of $[K^+]_o$-dependence of single-channel conductance between the previous studies and our data remain to be investigated. It is possible that the difference is attributable to the distinct systems employed. It may be noted that, for the single-channel studies of the gating and spermine blocking

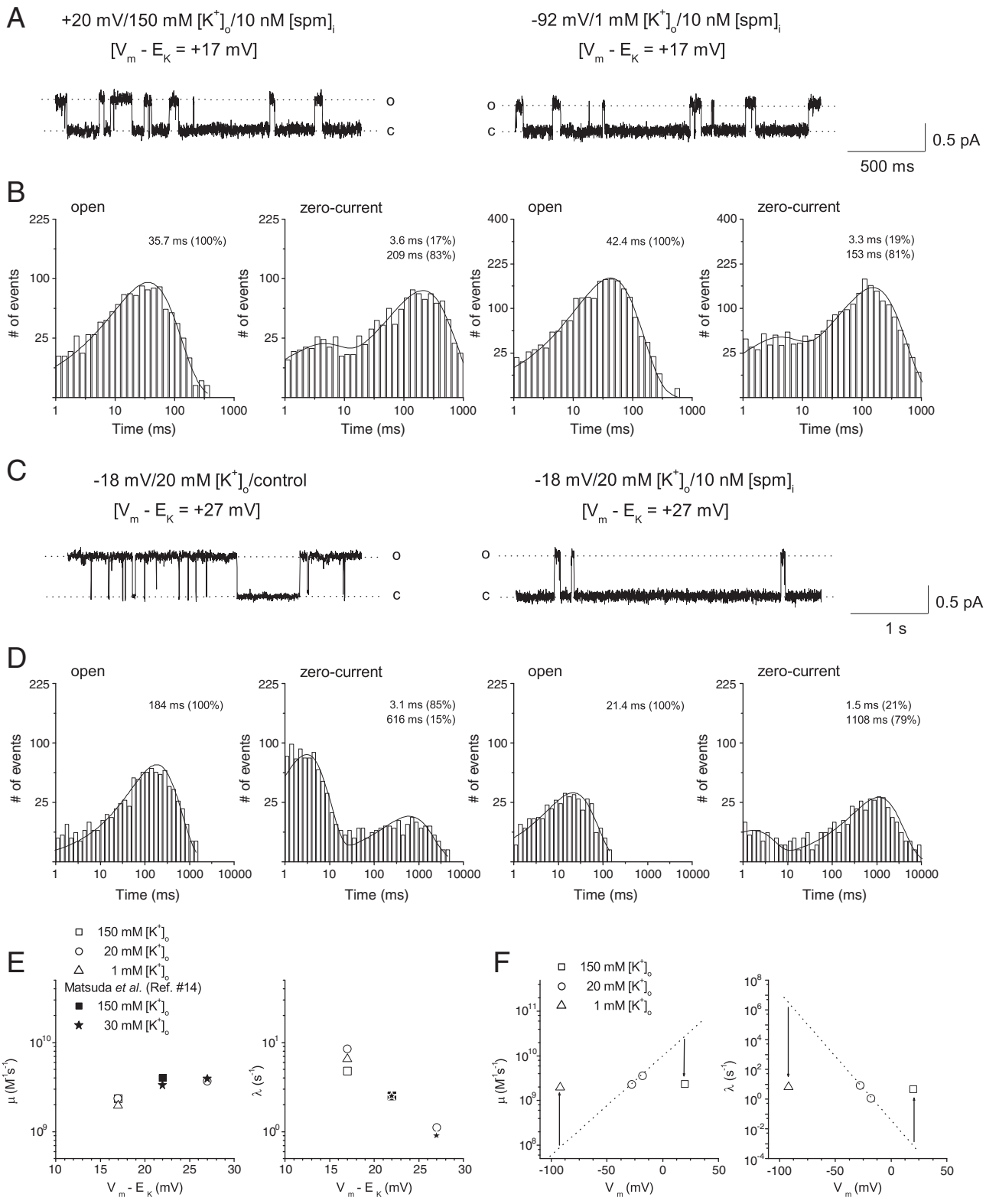

Fig. 5. Effects of $[K^+]_o$ on inhibition by intracellular spermine of outward i_{K1}. A. Single-channel currents recorded at 150 mM $[K^+]_o$ (left panel) and 1 mM $[K^+]_o$ (right panel) at 150 mM $[K^+]_i$ and a driving force = +17 mV in the presence of 10 nM [spermine]$_i$. B. The corresponding open and zero-current time distributions of single-channel currents. C. Single-channel currents recorded at 20 mM $[K^+]_o$ at 150 mM $[K^+]_i$ and $V_m = -18$ mV in the absence (left panel) and presence of 10 nM [spermine]$_i$ (right panel). D. The corresponding open and zero-current time distributions of single-channel currents. E. Effects of driving forces on μ and λ of the spermine block. The data reported by Matsuda et al., 2010 [6] are shown as closed stars square. F. Effects of V_m on μ and λ of the spermine block.

kinetics, the shallow $[K^+]_o$-dependence of outward single-channel current is advantageous in that it allows the kinetics to be examined at a broader $[K^+]_o$ range.

Previous studies [6,26,33] and our current work support the presence of an intrinsic gating mechanism (the C–O transition described in Scheme I) in the Kir2.1 channel. The gate is very likely

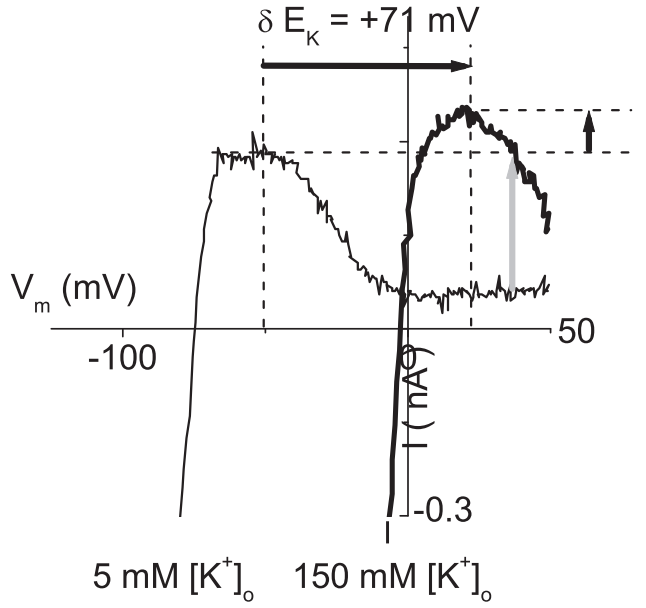

Fig. 6. Two major effects of $[K^+]_o$ on the I–V_m relationships of the Kir2.1 channels. I–V_m curves at $[K^+]_o = 5$ and 150 mV were the same as those shown in Fig. 1A. An increase of $[K^+]_o$ shifted the I–V_m relationships to the right (horizontal arrow) and increased the outward I_{K1} amplitude at a constant driving force value (black vertical arrow). The grey arrow indicates an increase of outward I_{K1} at a constant V_m when $[K^+]_o$ was changed.

located at the selectivity filter because changes in the amide carbonyls of G144 and G146 lining the filter affected the kinetics of single-channel gating [33]. It was proposed that conformational changes of the selectivity filter resulted from interaction of permeant ions and the backbone carbonyls, thus affecting gating [33]. In this study, we showed that the opening and closing rate constants increased to the same extent as the single-channel conductance when $[K^+]_o$ was increased, indicating that the intrinsic gating is regulated by $[K^+]_o$. However, this $[K^+]_o$ regulation of the intrinsic gate does not seem to be responsible for the $[K^+]_o$-dependence of outward I_{K1} because the open probability of the intrinsic gate is not affected by $[K^+]_o$.

4.4. Conclusion

Our results show that outward I_{K1} is larger at higher $[K^+]_o$ because single-channel conductance is increased at higher $[K^+]_o$ at a constant driving force. In addition, at a constant driving force, the open probabilities of the intrinsic gate and spermine-binding kinetics are the same at different values of $[K^+]_o$. This study supports that K^+ permeation regulated by $[K^+]_o$ as the new mechanism underlying the important modulation of outward I_{K1} by $[K^+]_o$. Outward I_{K1} plays a crucial role in maintaining the resting membrane potential, determining the excitation threshold, and initiating the final repolarization phase of the action potential. This study sheds light on the mechanism underlying the important regulation of outward I_{K1} by $[K^+]_o$.

Acknowledgments

We thank Dr Lily Jan for kindly providing the Kir2.1 clone. This work was supported by the Academia Sinica in Taiwan and the National Science Council of Taiwan (grant 98-2320-B001-009-MY3).

References

[1] S. Hagiwara, S. Miyazaki, N.P. Rosenthal, Potassium current and the effect of cesium on this current during anomalous rectification of the egg cell membrane of a starfish, J. Gen. Physiol. 67 (1976) 621–638.
[2] C.A. Leech, P.R. Stanfield, Inward rectification in frog skeletal muscle and its dependence on membrane potential and external potassium, J. Physiol. 319 (1981) 295–309.
[3] H. Matsuda, Effects of external and internal K^+ ions on magnesium block of inwardly rectifying K^+ channels in guinea-pig heart cells, J. Physiol. 435 (1991) 83–99.
[4] Y. Kubo, Effects of extracellular cations and mutations in the pore region on the inward rectifier K^+ channel IRK1, Recept. Channels 4 (1996) 73–83.
[5] A.N. Lopatin, C.G. Nichols, $[K^+]$ dependence of polyamine-induced rectification in inward rectifier potassium channels (IRK1, Kir2.1), J. Gen. Physiol. 108 (1996) 105–113.
[6] H. Matsuda, M. Hayashi, M. Okada, Voltage-dependent block by internal spermine of the murine inwardly rectifying K^+ channel, Kir2.1, with asymmetrical K^+ concentrations, J. Physiol. (2010).
[7] T.W. Claydon, S.Y. Makary, K.M. Dibb, M.R. Boyett, K^+ activation of kir3.1/kir3.4 and kv1.4 K^+ channels is regulated by extracellular charges, Biophys. J. 87 (2004) 2407–2418.
[8] P. Pennefather, C. Oliva, N. Mulrine, Origin of the potassium and voltage dependence of the cardiac inwardly rectifying K-current (IK1), Biohys. J. 61 (1992) 448–462.
[9] J. Lopez-Barneo, T. Hoshi, S. Heinemann, R. Aldrich, Effects of external cations and mutations in the pore region on C type inactivation of Shaker potassium channels, Recept. Channels 1 (1993) 61–71.
[10] L.A. Pardo, S.H. Heinemann, H. Terlau, U. Ludewig, C. Lorra, O. Pongs, W. Stuhmer, Extracellular K^+ specifically modulates a rat brain K^+ channel, Proc. Natl. Acad. Sci. U. S. A. 89 (1992) 2466–2470.
[11] T. Doi, B. Fakler, J.H. Schultz, U. Schulte, U. Brandle, S. Weidemann, H.P. Zenner, F. Lang, J.P. Ruppersberg, Extracellular K^+ and intracellular pH allosterically regulate renal Kir1.1 channels, J. Biol. Chem. 271 (1996) 17261–17266.
[12] H. Sackin, S. Syn, L.G. Palmer, H. Choe, D.E. Walters, Regulation of ROMK by extracellular cations, Biophys. J. 80 (2001) 683–697.
[13] U. Schulte, S. Weidemann, J. Ludwig, J. Ruppersberg, B. Fakler, K^+-dependent gating of K(ir)1.1 channels is linked to pH gating through a conformational change in the pore, J. Physiol. 534 (2001) 49–58.
[14] Y. Murata, Y. Fujiwara, Y. Kubo, Identification of a site involved in the block by extracellular Mg^{2+} and Ba^{2+} as well as permeation of K^+ in the Kir2.1 K^+ channel, J. Physiol. 544 (2002) 665–677.
[15] U. Ludewig, C. Lorra, O. Pongs, S.H. Heinemann, A site accessible to extracellular TEA^+ and K^+ influences intracellular Mg^{2+} block of cloned potassium channels, Eur. Biophys. J. 22 (1993) 237–247.
[16] O.P. Hamill, A. Marty, E. Heher, B. Sakmann, F.J. Sigworth, Improved patch-clamp techniques for high-resolution current recording from cells and cell-free membrane patches, Pflügers Arch. Eur. J. Physiol. 391 (1981) 85–100.
[17] D.W. Hilgemann, The giant membrane patch, in: B. Sakmann, E. Neher (Eds.), Single-Channel Recording, vol. 2, Plenum Press, New York, 1995, pp. 307–328.
[18] C.L. Huang, S. Feng, D.W. Hilgemann, Direct activation of inward rectifier potassium channels by PIP2 and its stabilization by Gbetagamma, Nature 391 (1998) 803–806.
[19] F.J. Sigworth, S.M. Sine, Data transformations for improved display and fitting of single-channel dwell time histograms, Biophys. J. 52 (1987) 1047–1054.
[20] B. Hille, Potassium channels and chloride channels, Ionic Channels of Excitable Membranes, 3, Sinauer, Sunderland, 2001, pp. 115–139.
[21] K. Ishihara, T. Mitsuiye, A. Noma, M. Takano, The Mg^{2+} block and intrinsic gating underlying inward rectification of the K^+ current in guinea-pig cardiac myocytes, J. Physiol. 419 (1989) 297–320.
[22] K. Ishihara, M. Hiraoka, Gating mechanism of the cloned inward rectifier potassium channel from mouse heart, J. Membr. Biol. 142 (1994) 55–64.
[23] P. Stanfield, N. Davies, P. Shelton, I. Khan, W. Brammar, N. Standen, E. Conley, The intrinsic gating of inward rectifier K^+ channels expressed from the murine IRK1 gene depends of voltage, K^+ and Mg^{2+}, J. Physiol. 475 (1994) 1–7.
[24] H.C. McKillen, N.W. Davies, P.R. Stanfield, N.B. Standen, The effect of intracellular anions on ATP-dependent potassium channels of rat skeletal muscle, J. Physiol. London 479 (1994) 341–351.
[25] A. Lopatin, E. Makhina, C. Nicols, Potassium channel block by cytoplasmic polyamines as the mechanism of intrinsic rectification, Nature 372 (1994) 366–371.
[26] H. Matsuda, K. Oishi, K. Omori, Voltage-dependent gating and block by internal spermine of the murine inwardly rectifying K^+ channel, Kir2.1, J. Physiol. 548 (2003) 361–371.
[27] D. Colquhoun, A.G. Hawkes, The principles of the stochastic interpretation of ion-channel mechanisms, in: B. Sakmann, E. Neher (Eds.), Single-Channel Recording, Plenum Press, New York, 1995, pp. 397–479.
[28] J.H. Morais-Cabral, Y. Zhou, R. MacKinnon, Energetic optimization of ion conduction rate by the K^+ selectivity filter, Nature 414 (2001) 37–42.
[29] Y. Zhou, J.H. Morais-Cabral, A. Kaufman, R. MacKinnon, Chemistry of ion coordination and hydration revealed by a K^+ channel–Fab complex at 2.0 Å resolution, Nature 414 (2001) 43–48.
[30] K. Ishihara, D.H. Yan, Low-affinity spermine block mediating outward currents through Kir2.1 and Kir2.2 inward rectifier potassium channels, J. Physiol. 583 (2007) 891–908.
[31] A.N. Lopatin, C.G. Nichols, $[K^+]$ dependence of open-channel conductance in cloned inward rectifier potassium channels (IRK1, Kir2.1), Biophys. J. 71 (1996) 682–694.
[32] D. Guo, Z. Lu, Mechanism of IRK1 channel block by intracellular polyamines, J. Gen. Physiol. 115 (2000) 799–814.
[33] T. Lu, A.Y. Ting, J. Mainland, L.Y. Jan, P.G. Schultz, J. Yang, Probing ion permeation and gating in a K^+ channel with backbone mutations in the selectivity filter, Nat. Neurosci. 4 (2001) 239–246.
[34] V. Carabelli, J.M. Hernandez-Guijo, P. Baldelli, E. Carbone, Direct autocrine inhibition and cAMP-dependent potentiation of single L-type Ca^{2+} channels in bovine chromaffin cells, J. Physiol. 532 (2001) 73–90.